Assimilating geomagnetic data into stochastic / deterministic quasi-geostrophic models of the Earth's outer core

Nicolas Gillet[1], Dominique Jault[1] and Chris Finlay[2]

(1) Institut des Sciences de la Terre, Grenoble, France (2) DTU Space, Copenhagen, Denmark

Geomagnetic data, from the Earth's surface to the core-mantle boundary

- continuous satellites records since 1999: global coverage ⇒ cleaner separation of internal and external sources
- observatories: continuous series, absolute intensities since 1840
- navigation: since late XVIth century, orientation only before 1840
- archeological artifacts and sediments: indirect records over the past 10,000 yrs

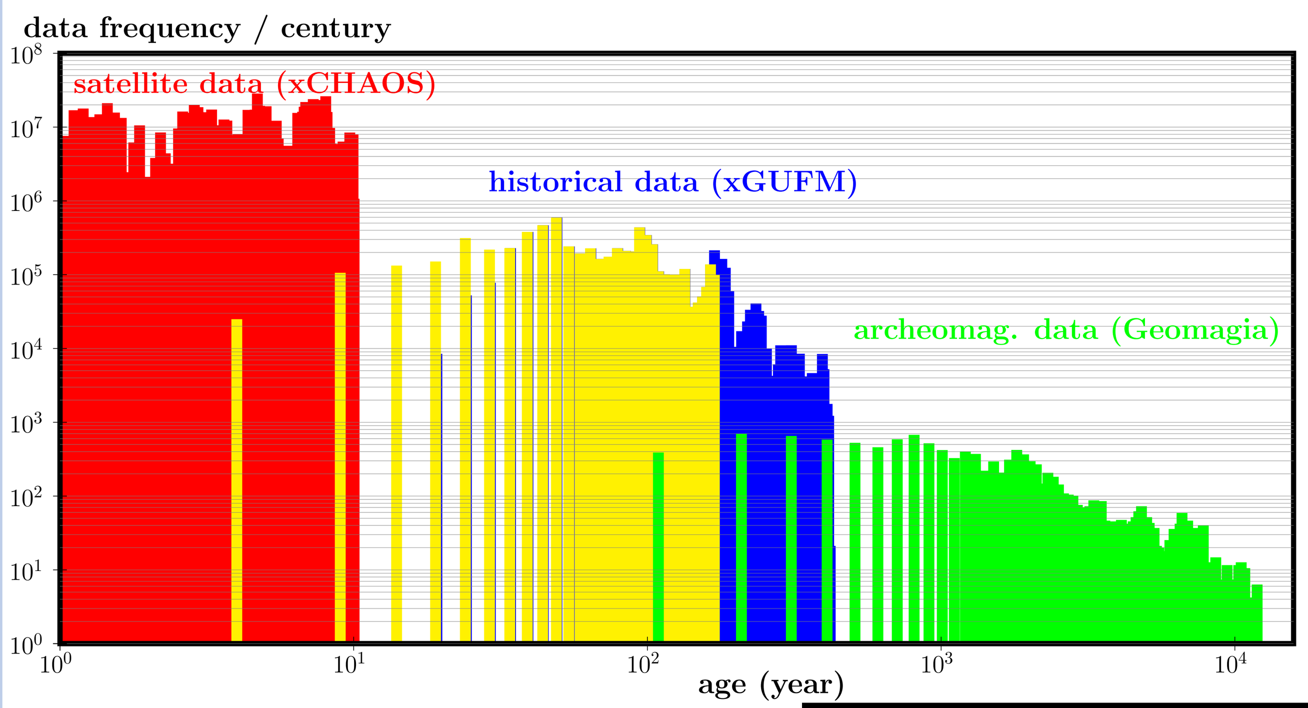

Fig. 1- data frequency from available databases of the archeomagnetic, historical, observatory and satellite era.

- Downward continuation through an electrically insulating mantle (Fig. 2) of noisy observations y^o at or above the Earth's surface
  - radial potential magnetic field B_r at the core surface:
    $$\boxed{y^o = \mathrm{H}(B_r) + e^o} \quad (1)$$
  - indirect measurements of the core state (ill-conditioned Green's functions in H)

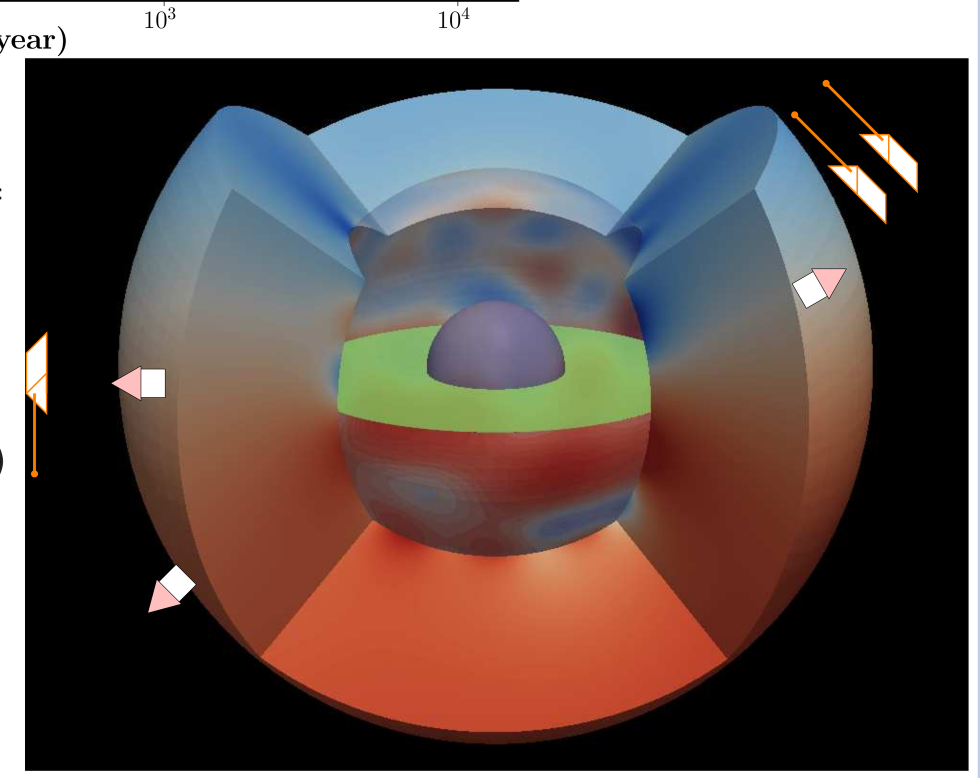

Fig. 2- From Fournier et al (2010)

Time-variable and time-correlated errors on the secular variation $\partial B_r/\partial t$

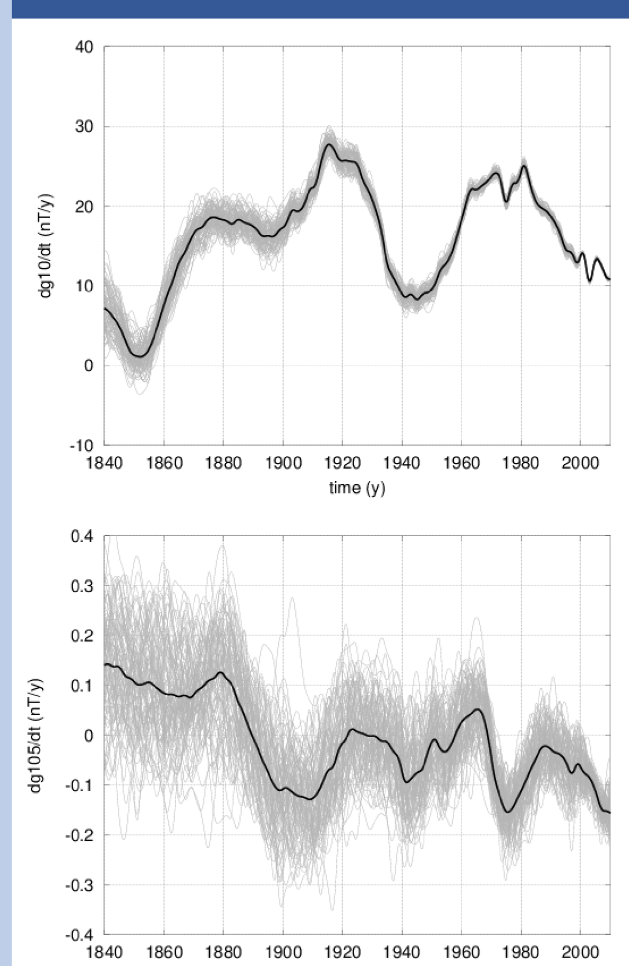

- Field changes related to horizontal core motions $\mathbf{u}_h$ through the core surface radial induction equation:
  $$\boxed{\frac{\partial B_r}{\partial t} = -\nabla_h \cdot (\mathbf{u}_h B_r) + \eta \nabla^2 B_r} \quad (2)$$
  with accuracy of the secular variation estimate depeding on both epochs and length-scales (Fig. 3)
- unresolved field features B_r' at small length-scales ($\ell < 800$ km at the core surface), with extrapolated decadal time-scales ⇒ time-correlated errors of representativeness (Gillet et al, 2009)
  $$\boxed{e^r = -\nabla_h \cdot (\mathbf{u}_h B r')} \quad (3)$$

Fig. 3- Ensemble of realizations of the secular variation spherical harmonic coefficients dg_1^0/dt (top) and dg_{10}^5/dt (bottom), in nT/yr, with the average value in black (from Gillet et al, submitted).

Geomagnetic power spectrum $S(f)$ and stochastic modeling

- Observed series suggest the process X sampled by geomagnetic records is:
  - $\mathcal{C}^0$ (continuous, not differentiable) on centenial periods and longer (Fig. 5)
  - $\mathcal{C}^1$ (continuous, once differentiable) from 5 to 100 yrs periods (Fig. 6)
- spectral densities (Fig. 4) are compatible with Auto-Regressive (AR) processes and stochastic differential equations (below W stands for a white noise process)

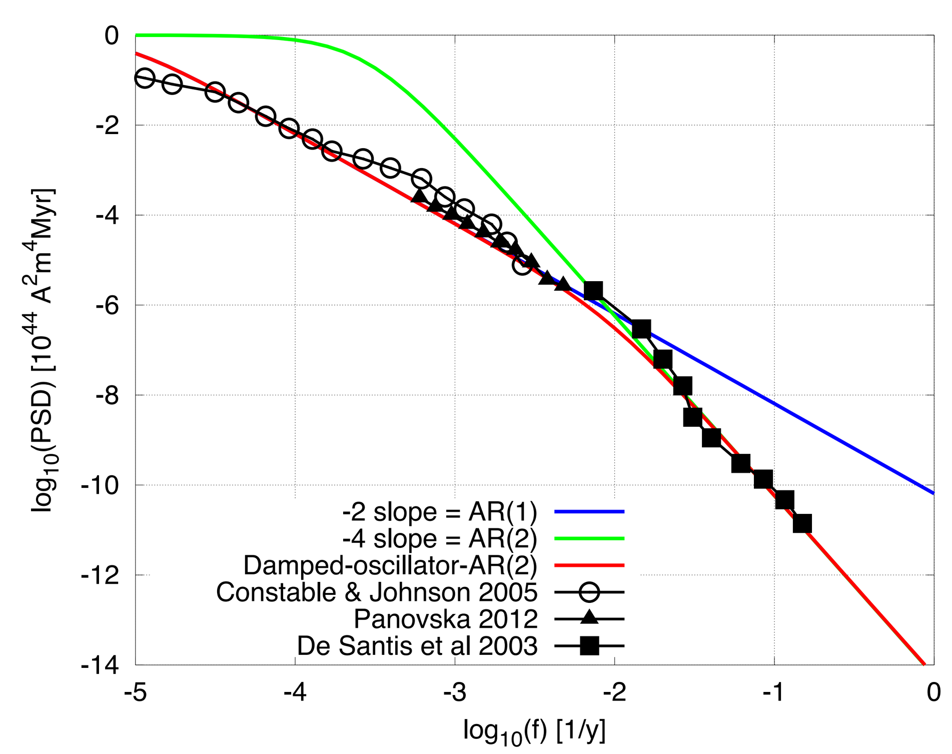

Fig. 4- Composite power spectral density (PSD) for several geomagnetic series, superimposed with that of some AR processes.

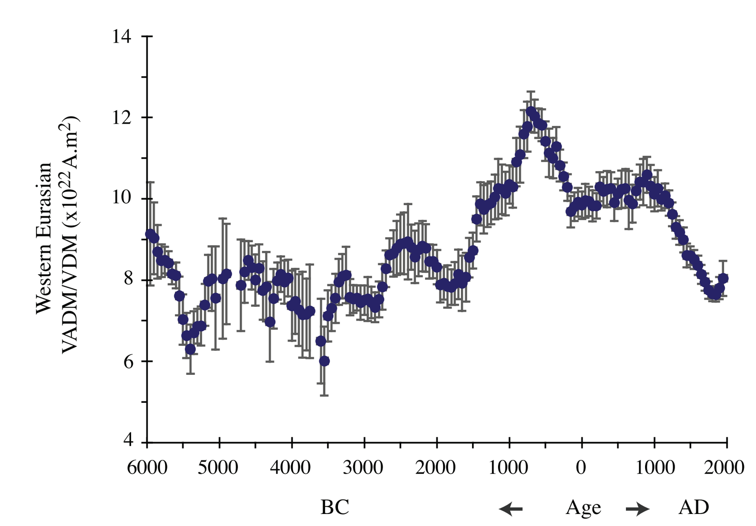

Fig. 5- Virtual axial dipole moment (VADM) from archeomagnetic records (Genevey et al, 2008).

- $100 - 10^5$ yrs periods: $S(f) \propto f^{-2}$
  - AR-1 process with $\tau_1 \sim 20,000$ yrs, e.g.
    $$\frac{\partial X}{\partial t} + \frac{X}{\tau_1} = W \,,$$
  - if valid for the dipole (Fig. 5), is it still the case for smaller length-scales?
- $5 - 100$ yrs periods: $S(f) \propto f^{-4}$
  - AR-2 process with $\tau_2 \sim 1000$ yrs, e.g.
    $$\frac{\partial^2 X}{\partial t^2} - \frac{3X}{\tau_2^2} = W \,.$$
  - ⇒ the induction equation (2) suggests the flow is governed by an AR-1 stochastic differential equation of the form
    $$\boxed{\frac{\partial \mathbf{u}_h}{\partial t} + \frac{\mathbf{u}_h}{\tau_u} = \mathbf{w}} \quad (4)$$

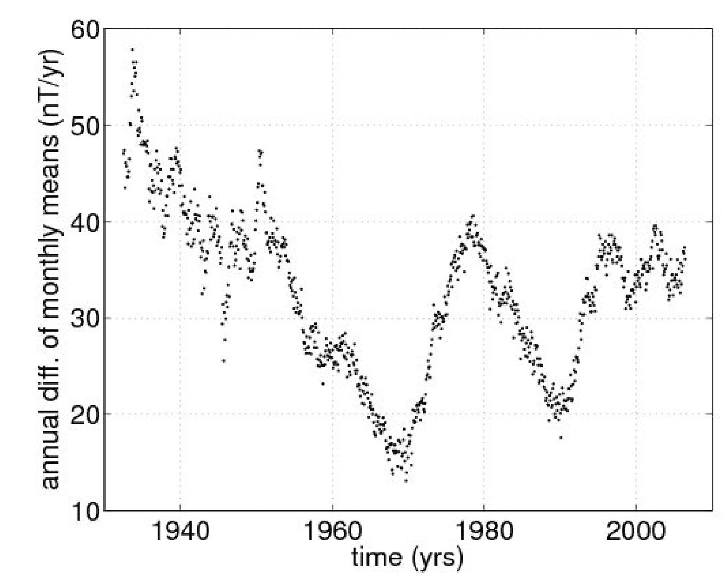

Fig. 6- Eastward component of $d\mathbf{B}/dt$ at the Niemegk observatory (Germany).

- aim at coupling (2) and (4) with an Ensemble Kalman Smoother (Evensen & Van Leeuwen, 2000), using an state augmentation approach (e.g. Reichle et al, 2002) to account for time-correlated errors in equation (3).
  This is made possible by the small size of this problem, $\mathcal{O}(500)$ parameters / epoch.
- NB: instantaneous flow accelerations are meaningless in this framework, only flow increments between two epochs make sense.

References

- Canet, Fournier & Jault, J. Geophys. Res. 114, B11101, doi:10.1029/2008JB006189, 2009.
- Evensen & Van Leeuwen, Mon. Weather Rev. 128, 1852–1867, 2000.
- Fournier et al, Space Sci. Rev. 155, 247-291, 2010.
- Fournier, Aubert and Thébault, Geophys. J. Int 186, 118–136, 2011.
- Genevey et al, Geochem. Geophys. Geosyst. 9, Q04038, doi:10.1029/2007GC001881, 2008.
- Gillet, Jault, Finlay & Olsen, submitted to Geochem. Geophys. Geosyst..
- Gillet, Jault, Canet & Fournier, Nature 465, 74–77, 2010.
- Gillet, Pais & Jault, Geochem. Geophys. Geosyst. 10, Q06004, doi:10.1029/2008GC002290, 2009.
- Jault, Phys. Earth Planet. Int. 166, 67–76, 2008.
- Li, Livermore & Jackson, Phys. Rev. E 84, 056321, doi:10.1103/PhysRevE.84.056321, 2011.
- Liu, Tangborn & Kuang, J. Geophys. Res. 112, B08103, doi:10.1029/2006JB004691, 2007.
- Reichel, McLaughlin & Entekhabi, Mon. Weather Rev. 130 , 103–114, 2002.

Sampling rate of the core state

- high sampling rate in modern (observatories and satellite) data, but...
  - 6 months day-time (i.e. noisy) data at high latitudes: fake global coverage
  - ambiguity between core and external (magneto- and ionospheric) sources
  - mantle conductivity = low-pass filter: which cut-off frequency?
- monthly to interannual periods:
  - shall we extrapolate the AR-2 process at periods below $\mathcal{O}(1)$ year?
  - should the process be different at periods shorter than the 4 yrs period of deterministic torsional (i.e. zonal and geostrophic) Alfvén waves, responsible for length-of-day (LOD) changes at 6–9 yrs periods (after Gillet et al 2010) ?

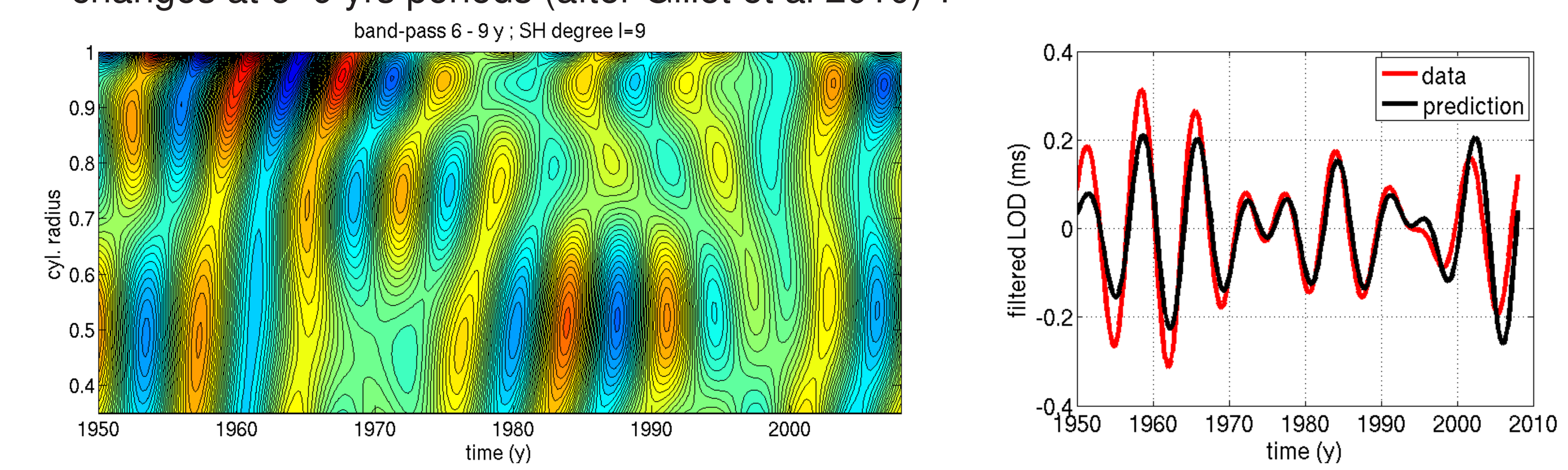

Fig. 7- Torsional Alfvén waves (left), as detected from observatory records, travelling from the inner core (s = 0.35) to the equator of the outer core (s=1), and their 6–9 yrs band-pass signature (right) on the LOD changes compared to the observations.

Imaging magnetic forces inside the core with a deterministic model?

- 3-dimensional sequential (Liu et al, 2007; Fournier et al, 2011) and variational (Li et al, 2011) attempts at estimating the core state, but filter out rapid variations
- in the Earth's core: inertial waves period $\tau_i \ll$ magnetic Afvén waves period $\tau_a \ll$ magnetic diffusion time τ_d
  - ⇒ large length-scale transient motions invariant along the rotation axis $\mathbf{e}_z$ (Jault, 2008), cf. Lehnert number
    $$\lambda = \tau_i/\tau_a \sim 10^{-4} \,.$$
  - ⇒ weak magnetic diffusion at large length-scales, as measured by the Lundquist number
    $$S = \tau_d/\tau_a \sim 10^5 \,.$$
- motivates a diffusiveless quasi-geostrophic model for z-invariant equatorial motions (following Canet et al, 2009)
  $$\mathbf{u}_e(s, \phi, t) = \mathbf{e}_z \times \nabla\psi \,,$$
  and the z-averaged quadratic quantities
  $$\mathbf{q} = \frac{1}{2H}\int_{-H}^{H} \left[B_s^2, B_\phi^2, B_s B_\phi\right] dz \,,$$
  with $H(s)$ the half-height of a fluid column, and $\beta(s) \propto \dfrac{1}{\lambda}\dfrac{dH}{ds}$ the coriolis parameter:
  $$\boxed{\beta\frac{\partial^2\psi}{\partial t \partial\phi} = \mathcal{F}(\psi, \mathbf{q})} \quad (5)$$
- coupling eqns (1), (2) and (5) using an EnKF
  - to obtain a first image of magnetic forces $\mathbf{q}$:
  - to forecast the field evolution (candidate to the International Geomagnetic Reference Field)

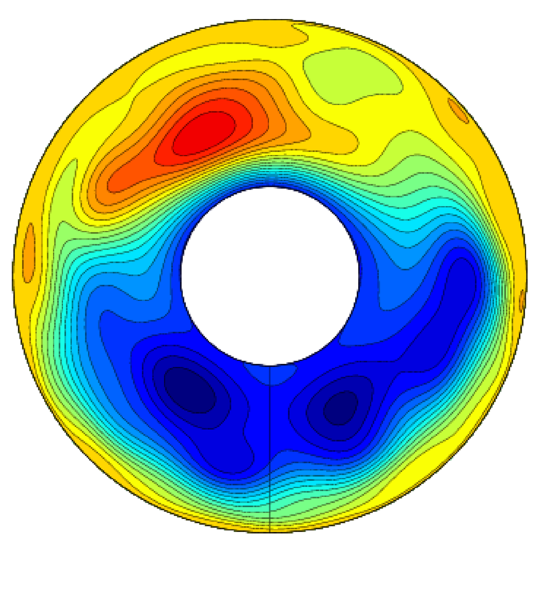

Fig. 8- Example of equatorial maps for ψ (top) and $d\psi/dt$ (bottom) obtained from satellite data in 2005 and equation (2), after Gillet et al (2009).

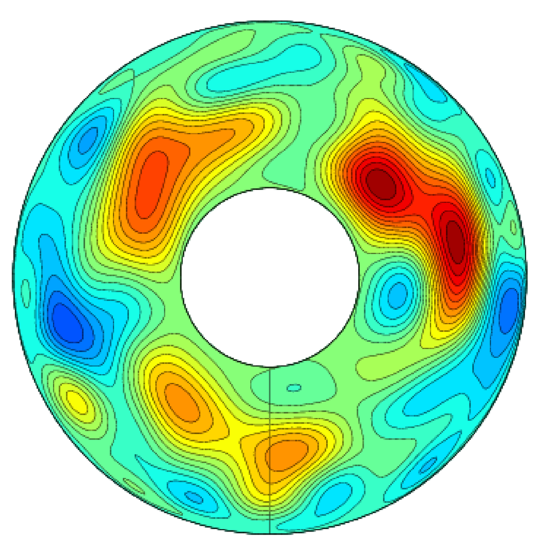

(a) must account for large uncertainties on ψ, even more on $\partial_t\psi$
(b) favored by a suspected steep spatial power spectrum for $\mathbf{q}$
(c) bounded value problem (positiveness + Cauchy-Schwartz constraint on the unknown $\mathbf{q}$)
(d) reconcile stochastic constraint (4) with (5): consider flow increments instead of $\partial_t\psi$.

Mail: nicolas.gillet@ujf-grenoble.fr